PTEP

Prog. Theor. Exp. Phys. **2024** 023G01(ptae017)
DOI: 10.1093/ptep/ptae017

Heavy Ion Injection of Fixed-Field Alternating Gradient Accelerator

Yujiro Yonemura[1,*], Hidehiko Arima[1], Hiroki Nishibata[2], Takashi Teranishi[2], Tomotsugu Wakasa[2], Nobuo Ikeda[1], Kenichi Watanabe[1], Nobuhiro Shigyo[1], Tatsunori Iwamura[2], Kyosuke Adachi[1], Koki Takamatsu[1], Motoki Kotani[2], Hisato Tanaka[2], Rintaro Matsunaga[2], Taichi Matsumoto[2], Kyohei Takenaka[2], Takafumi Kajihara[2], Sotaro Matsunaga[2], Yusuke Shinohara[2], and Yoshiharu Mori[3]

[1]*Department of Engineering, Kyushu University, 744, Motooka, Nishi-ku, Fukuoka City, Fukuoka 819-0395, Japan*
[2]*Department of Physics, Kyushu University, 744, Motooka, Nishi-ku, Fukuoka City, Fukuoka 819-0395, Japan*
[3]*Institute for Integrated Radiation and Nuclear Science, Kyoto University, 2, Asashiro-Nishi, Kumatori-cho, Sennan-gun, Osaka 590-0494, Japan*
*Email: ynmr@nucl.kyushu-u.ac.jp

Received April 19, 2023; Accepted January 25, 2024; Published January 27, 2024

Much research in recent years has focused on circular accelerators that accelerate and store secondary particles with a large momentum spread, such as muons, unstable nuclei, and heavy ions with different charge states. A fixed-field alternating gradient (FFAG) accelerator with large transverse and momentum acceptance has obvious advantages for such requirements. A versatile beam injection method is required to accelerate secondary particles with a large momentum spread and different charge states with an FFAG accelerator. In the present study, a method for charge exchange injection of positive heavy ions using the large momentum acceptance of an FFAG accelerator is proposed. A charge injection system, which converts a He^{1+} beam to a He^{2+} beam, is developed for a 150 MeV FFAG accelerator at the Center for Accelerator and Beam Applied Science (CABAS) of Kyushu University. As the first step to verify the injection method, an orbit shift from one charge state to the other is demonstrated. This is the first demonstration of heavy ion injection using an FFAG accelerator.

Subject Index G02, G05

1. Introduction

Much research in recent years has focused on circular accelerators that accelerate and store secondary particles with a large momentum spread, such as muons, unstable nuclei, and heavy ions with different charge states [1–3]. A fixed-field alternating gradient (FFAG) accelerator with large transverse and momentum acceptance has obvious advantages for such requirements.

The concept of the FFAG accelerator was originally proposed in 1953 [4]. Electron models of the FFAG accelerator were constructed in the early 1960s [5]. The world's first proton FFAG accelerator (PoP-FFAG) was developed at the High Energy Accelerator Research Organization (KEK) in 2000 [6]. A 150 MeV FFAG accelerator, which is a prototype machine for applications such as proton cancer therapy, has been developed based on the results of PoP-FFAG's development [7]. Following such successes, various types of FFAG accelerators have been

developed at many institutes [8]. However, an FFAG accelerator to accelerate heavy ions has not yet been developed.

A versatile beam injection method is required to accelerate secondary particles with a large momentum spread and different charge states using an FFAG accelerator. A charge exchange injection method is widely used in conventional synchrotrons, including FFAG accelerators. In this method, the injected negative ions are converted to positive ions using a charge-stripping carbon foil. A charge exchange injection system for a H^- beam has already been developed for an FFAG accelerator [9–11]. The multiturn injection method is employed for positive ions in conventional synchrotrons and FFAG accelerators [12]. However, in principle, the efficiency of multiturn injection is low compared to that for the charge exchange injection method. In addition, to inject ion beams with different momenta and charge states, the operation conditions and positions of injection equipment such as pulsed bump magnets must be varied to match the injected ion beams.

In this study, a method for charge exchange injection of positive heavy ions using the large momentum acceptance of an FFAG accelerator is proposed. A charge injection system, which converts a He^{1+} beam to a He^{2+} beam, is developed for a 150 MeV FFAG accelerator at the Center for Accelerator and Beam Applied Science (CABAS) of Kyushu University. As the first step to verify the injection method, an orbit shift from one charge state to the other is demonstrated.

2. Accelerator facility at Kyushu University

In order to promote activities in all scientific, medical, engineering, and educational fields related to the application of accelerators and radiation, CABAS was established at Kyushu University. To achieve the purpose of the center, Kyushu University decided to construct a new facility that merges three institutes, the Cockcroft-Walton Accelerator Laboratory of the Faculty of Engineering, the Institute for Irradiation and Analysis of Quantum Radiations, and the Kyushu University Tandem Accelerator Laboratory of the Faculty of Science, on its new campus (Ito Campus). Figure 1 shows an overview of the new accelerator facility at Kyushu University. The facility consists mainly of a 10 MeV proton cyclotron, an 8 MV tandem accelerator, and a 150 MeV FFAG accelerator as a replacement of the Cockcroft-Walton accelerator.

The 150 MeV FFAG accelerator was developed at KEK as a prototype of a proton FFAG accelerator for applications such as proton beam therapy. The main parameters for the 150 MeV FFAG accelerator are summarized in Table 1. Beam extraction with 100 Hz operation was successfully demonstrated in 2005 [13]. The FFAG accelerator was disassembled in 2006 and transported by land from KEK to Kyushu University in 2008. Reconstruction of the FFAG accelerator began at CABAS in 2008. Beam commissioning was started in 2011, and beam acceleration was successfully demonstrated in 2013.

The tandem accelerator has been employed independently for accelerator mass spectrometry, student experiments, radio-isotope beam production, and low-energy nuclear physics experiments. The tandem accelerator is employed as a heavy ion injector for the 150 MeV FFAG accelerator. Construction of the tandem accelerator and experimental rooms was completed in 2013. Beam commissioning of the tandem accelerator began in 2014.

A beam transport line, which delivers a heavy ion beam from the tandem accelerator to the FFAG accelerator, was constructed to demonstrate the injection and acceleration of a heavy ion beam for the FFAG accelerator.

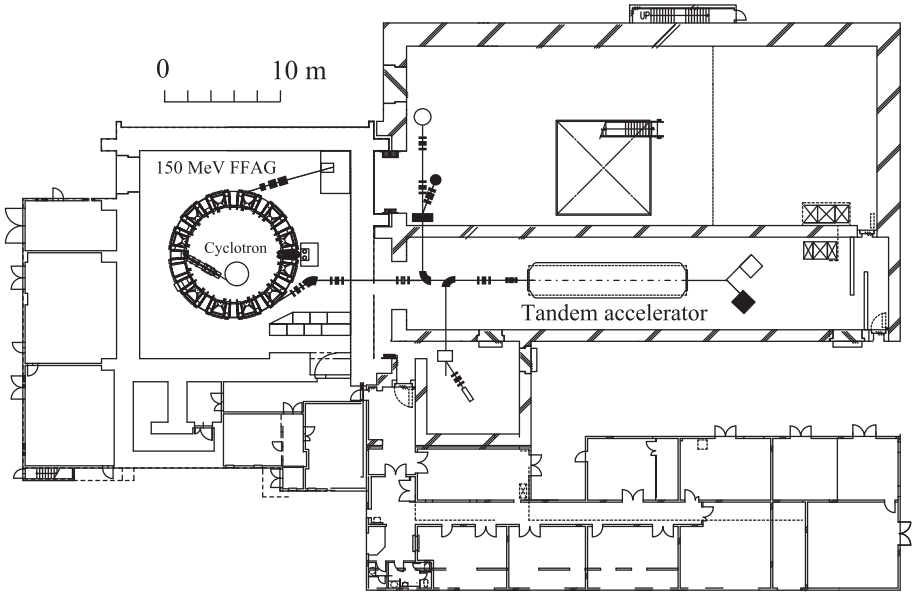

Fig. 1. Layout of CABAS of Kyushu University [14].

Table 1. Design parameters for the 150 MeV FFAG accelerator.

Magnet type	Radial sector (DFD triplet)
Number of cells	12
Proton energy (MeV)	10–125
Average radius (m)	4.47–5.20
Revolution frequency (MHz)	1.5–4.6
Field index	7.65
Magnetic rigidity (Tm)	0.46–1.67
Dispersion function at center of straight section (m)	0.6
Beta function at center of straight section (m)	1.0 (Horizontal) 4.4 (Vertical)
Betatron tune	3.61 (Horizontal) 1.46 (Vertical)

3. Charge-stripping injection for heavy ion beam acceleration

Conventionally, the multiturn injection method is often employed for positive ions in synchrotrons, including FFAG accelerators. In this study, a charge exchange injection method for positive heavy ions using the large momentum acceptance of the FFAG accelerator is proposed. In this injection method, the charge state of the injected positive ions is made more positive using a charge-stripping foil.

Since the FFAG accelerator satisfies the scaling condition, the closed orbit corresponding to the momentum and charge state of a particle is uniquely determined, and they have geometrical similarity. In principle, positive heavy ions which satisfy the following conditions can be injected and accelerated without changing the magnetic field: the revolution frequency of the heavy ions is within the frequency bandwidth of the radiofrequency (RF) cavity, and the magnetic rigidity of the injected and circulating heavy ions is within the range of the magnet.

In this study, a He ion beam is employed to demonstrate the injection of a heavy ion beam. A schematic diagram of the injection system for a heavy positive ion beam is shown in Fig. 2.

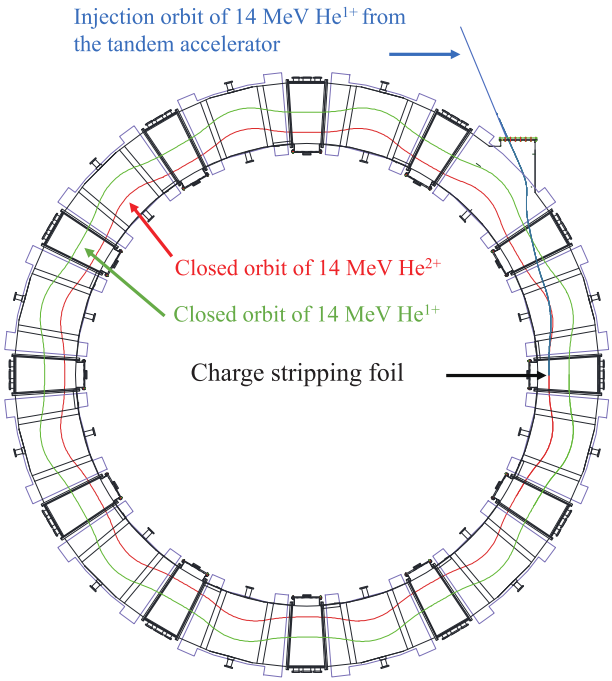

Fig. 2. Injection orbit of He^{1+} (blue line), closed orbit of He^{1+} (green line), and closed orbit of He^{2+} (red line). The charge-stripping foil is installed at the intersection of the injection orbit and the closed orbit of He^{2+}.

As the injector to the FFAG accelerator, the tandem accelerator is employed. He^- ions were extracted from the ion source and accelerated to 7 MeV. The electrons are stripped by Ar charge-stripping gas at the center of the tandem accelerator. Although all electrons are normally stripped and He^- ions are converted to He^{2+} ions with the tandem accelerator, He^- ions are converted to He^{1+} ions for the proposed injection method since the charge state will be further increased by the foil in the FFAG accelerator. The He^{1+} beam is reaccelerated to 14 MeV and injected into the FFAG accelerator. The He^{1+} beam is then converted to a He^{2+} beam by the charge-stripping foil.

To determine the closed orbit of the He^{2+} beam and the injection orbit of the He^{1+} beam, 3D particle tracking using Runge–Kutta integration is performed. The distribution of the magnetic field was calculated with OPERA-3D [15]. The magnetic rigidity of a 14 MeV proton is 0.54 Tm, which is approximately equal to a 14 MeV He^{2+} beam. The currents in the coils of the focusing magnet and defocusing magnet are 44,170 AT and 5,500 AT, respectively, which are the same conditions used for proton beam acceleration from 10 to 100 MeV. The injection orbit was determined by back tracking from the foil location.

Since the energy of an injected beam is 3.5 MeV/u, which is relatively low, a thin stripping foil is required. For beam acceleration, the energy lost in the foil can be recovered by RF acceleration. To allow the beam to escape from the stripping foil, orbit shift by acceleration can be used in the FFAG accelerator [16]. In this method, the beam is accelerated and stacked simultaneously and no injection devices such as bump magnets for injection are needed. A 10 $\mu g/cm^2$ carbon foil, which is the minimum thickness that can be manufactured in the facility, is assumed to be employed as the charge-stripping foil in the present study, which produces a mean energy loss for a 14 MeV He beam of about 4 keV [17].

Table 2. Parameters for injection and acceleration.

Particle	He^{2+}
Charge-stripping foil	carbon
Foil thickness (μg/cm^2)	$t = 10$
Foil dimensions (mm)	$w = 15$ (width), $h = 35$ (height)
Stopping power for 14 MeV He^{2+} ions (MeV/g/cm^2)	$S = 3.76 \times 10^2$
RF voltage (kV)	$V_0 = 6.0$
RF acceleration phase (degrees)	$\phi_s = 30$
Harmonic number of RF acceleration	1

4. Estimation of emittance growth and energy spread for charge-stripping injection

Electron stripping by a thin carbon foil is used to convert He^{1+} to He^{2+} ions. Here, we estimate the beam emittance growth and energy spread during the beam injection process. The typical parameters used in the beam injection and acceleration scheme are described below.

The energy gain for one-turn passage through the foil is given by

$$\Delta E = qV_0 \sin\phi_s - \Delta E_s. \tag{1}$$

Here, q, V_0, ϕ_s, and ΔE_s are the charge state of particles, the RF voltage, the RF acceleration phase, and the energy loss in the stripping foil, respectively.

The horizontal beam shift at the stripping foil for one-turn acceleration can be obtained by

$$\Delta x = \eta\frac{\Delta p}{p} = \frac{\eta}{\beta^2}\frac{\Delta E}{E}, \tag{2}$$

where η, p, β, and E are the dispersion function at the injection point, the momentum, the relativistic velocity, and the total energy, respectively.

The total number of turns passing through the stripping foil region is thus given by

$$N = \frac{w}{\Delta x} = \frac{w\beta^2 E}{\eta(qV_0 \sin\phi_s - \Delta E_s)}. \tag{3}$$

Here, w is the width of the foil. When the values listed in Tables 1 and 2 are substituted into Eq. (3), the total number of turns becomes:

$$N \simeq 310 \text{ turns}. \tag{4}$$

This multitraverse beam process resembles an ionization cooling system where particles pass through a medium and the energy loss through ionization is recovered by RF acceleration. Evaluation of the growth of beam emittance and energy spread during this process is required for efficient beam injection. The transverse emittance growth depends mostly on coulombic multiple scattering in this region; therefore, the emittance growth can be evaluated by the following rate equation [18,19]:

$$\frac{d\epsilon_t}{ds} = -\frac{S(E)}{\beta^2 E}\epsilon_t + \frac{\beta\gamma\beta_T}{2L_s}\left(\frac{13.6 \text{ MeV}}{\beta cp}\right)^2, \tag{5}$$

where $S(E)$, γ, β_T, L_s, s, p, and c are the stopping power, the Lorentz factor, the beta function at the injection point, the radiation length, momentum, and the velocity of light, respectively. On the other hand, the growth of a longitudinal energy spread σ_E as a function of the target thickness can be evaluated by the following rate equation:

$$\frac{\langle\sigma_E^2\rangle}{ds} = -2\frac{\partial S(E)}{\partial E}\langle\sigma_E^2\rangle + 4\pi(r_e m_e c^2)^2 n_e \gamma^2\left(1 - \frac{\beta^2}{2}\right), \tag{6}$$

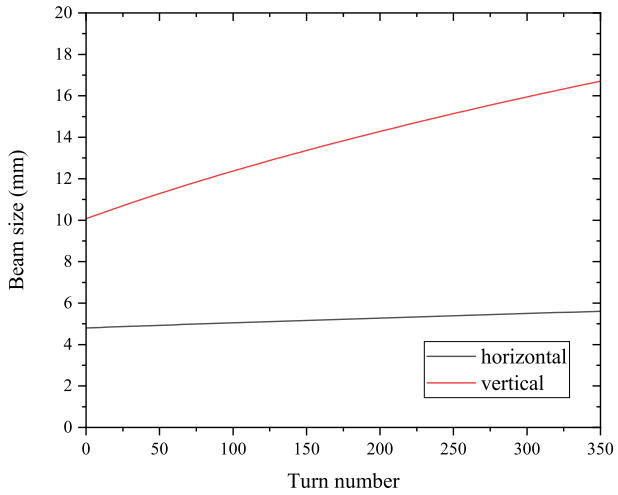

Fig. 3. Beam size as a function of turn number.

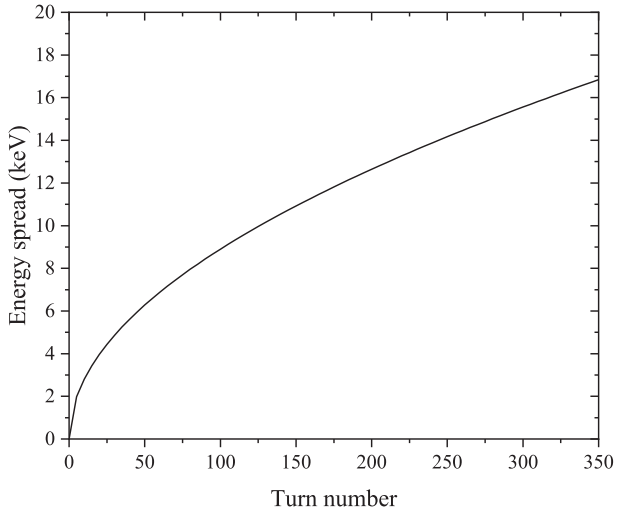

Fig. 4. Energy spread as a function of turn number.

where r_e is the classical electron radius, m_e is the rest mass of an electron, and n_e is electron density.

The beam half width $\sqrt{\epsilon_t \beta_T}$ and the longitudinal energy spread were estimated based on ionization cooling theory; the results are shown in Figs. 3 and 4, respectively. The size, angular, and energy spread of the extracted beam from the tandem accelerator are expected to be approximately ±2 mm, ±4 mrad, and 0.1%, respectively. The initial normalized emittance and energy spread are assumed to be 2 mm mrad and zero, respectively.

Figure 3 shows that the horizontal and vertical beam sizes were 6 mm and 16 mm, respectively, when injection was complete. The vertical beam size was 2.7 times larger than the horizontal beam size since the vertical beta function is 4.4 times larger than the horizontal beta function at the center of the straight section, as shown in Table 2. The minimum required width and height of the carbon foil were approximately 12 mm and 32 mm, respectively.

Figure 4 shows that the energy spread after beam injection was estimated to be approximately 15 keV. The half RF bucket size of the FFAG accelerator under the conditions of Table 2

is approximately 290 keV; therefore, the estimated energy spread is sufficiently small to allow stable beam injection and acceleration.

Since a continuous beam is injected from the tandem accelerator, beam loss occurs when RF acceleration is employed [20]. The phase acceptance range is from −39 to 150 degrees when the acceleration phase is 30 degrees. Therefore, the efficiency of beam capture and acceleration is estimated to be less than 52% when the continuous beam is injected from the tandem accelerator. To increase the injection efficiency, the time width of the beam must be bunched using an electric beam chopper installed in the injection line.

5. Experimental setup

A beam experiment with the tandem accelerator and the FFAG accelerator was performed at CABAS to evaluate the effectiveness of the injection method. This experiment was performed to demonstrate the part of the beam injection method that relates to charge exchange injection without RF acceleration. The acceleration of heavy ions is limited due to the present radiation safety restrictions of the facility.

The He beam injection system was developed based on the particle tracking results. The layout of the beam injection line from the tandem accelerator and the position of the charge-stripping foil were also determined. A 14 MeV He^{1+} beam was extracted and transported from the tandem accelerator to the FFAG accelerator. The mean beam current was 0.7 nA. In the matching section of the beam transport line, two steering magnets, two bending magnets, and six quadrupole magnets were employed to adjust the beam positions and the beam profiles. In this study, matching of the beta function between the FFAG accelerator and the tandem accelerator is not performed since the large leakage field including the nonlinear magnetic field disturbs the magnetic field at the injection position.

Figure 5 shows a schematic of the beam injection system, which consists of a movable charge-stripping foil and three ceramic fluorescent screens. The fluorescent screens, which are tilted 45° to the beam orbit, are observed by a charge-coupled device (CCD) camera from outside of a viewport mounted on the vacuum chamber. These 50 mm wide, 50 mm high, and 5 mm thick screens are employed to observe the profile and position of the injected beam. Figure 5 shows fluorescent screen A, which is installed at the end of the beam transport line from the tandem accelerator. The radially movable fluorescent screen B is installed outside of the FFAG accelerator at the straight section.

Figure 6 shows a schematic illustration and a photograph of the charge-stripping foil, which is mounted on a motorized linear motion feed-through. The horizontal range of motion is 900 mm, and accuracy of the position is 1 mm.

Since charge exchange injection without beam acceleration was performed in this experiment, it was not necessary to employ the large, thin foil. A 50 $\mu g/cm^2$ thick carbon foil, which has high mechanical strength and is easily manufactured, was employed since a 10 $\mu g/cm^2$ thick carbon foil is brittle and sensitive handling is required. The stripping efficiency for 14 MeV He ions is approximately 94% for the 50 $\mu g/cm^2$ thick foil [21]. The width and height of the carbon foil were 10 mm and 10 mm, respectively. Larger foils required for beam acceleration are currently being manufactured. Figure 6 shows a schematic illustration of the ceramic fluorescent screen C mounted at a distance of 10 mm from the foil in the radial direction.

A destructive beam profile monitor and radial beam probe were employed to measure the profile of the injected He^{2+} beam. The destructive beam profile monitor consists of a copper

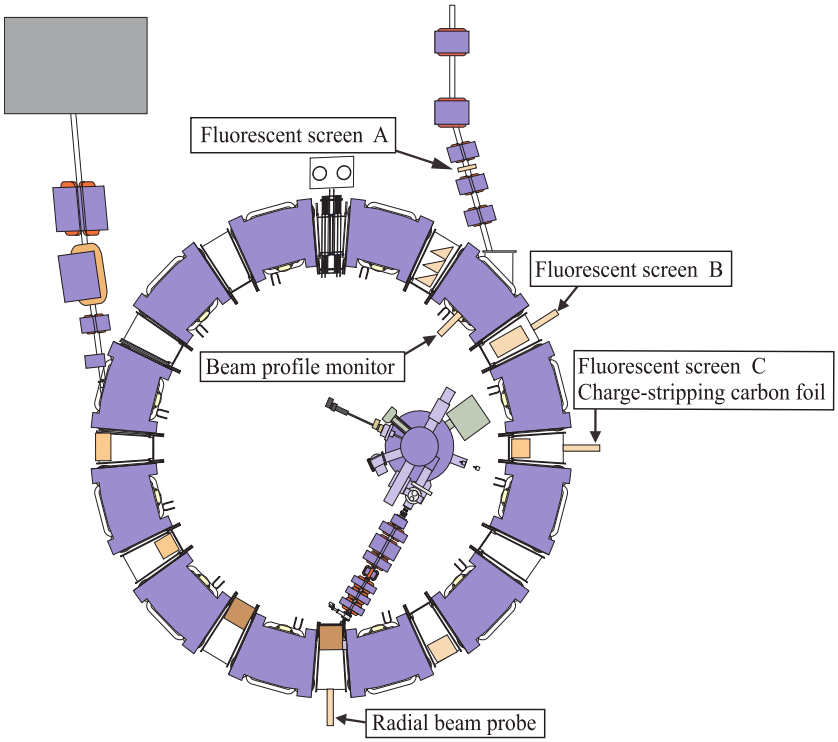

Fig. 5. Schematic of injection system and beam diagnostics.

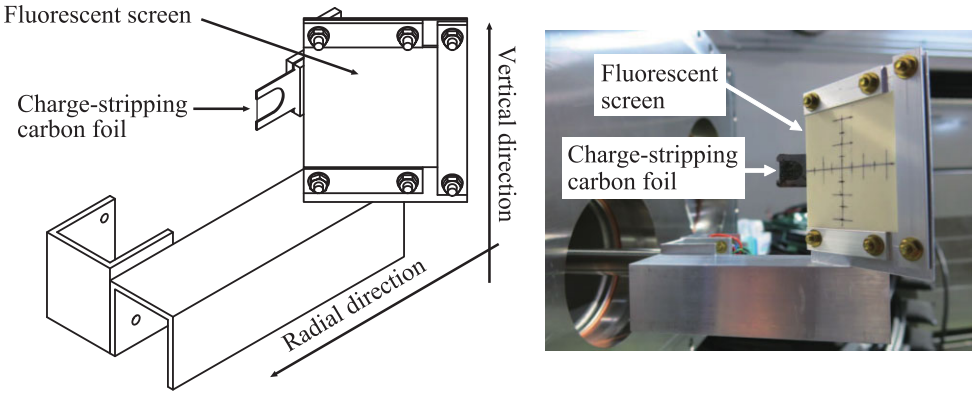

Fig. 6. Schematic illustration and photograph of the charge-stripping foil and fluorescent screen layout.

electrode and a motorized cylinder mounted inside the vacuum chamber of the accelerator. The position of the beam profile monitor is moved stepwise along the radial axis. The range of movement and positional accuracy were 300 mm and 0.2 mm, respectively. The electrode is moved at regular intervals, and the beam current is measured at each position. The time series data of measured current provide the average current and statistical error. The position intervals, the sampling time, and the number of samples at each position are 1 mm, 0.1 seconds, and 50, respectively.

The radial beam probe was a movable destructive current monitor designed to measure the beam current along the radial axis. A copper electrode was mounted at the end of a motorized stainless-steel rod outside the vacuum chamber. The range of movement and positional accuracy of the electrode were 900 mm and 1 mm, respectively. The beam current was measured

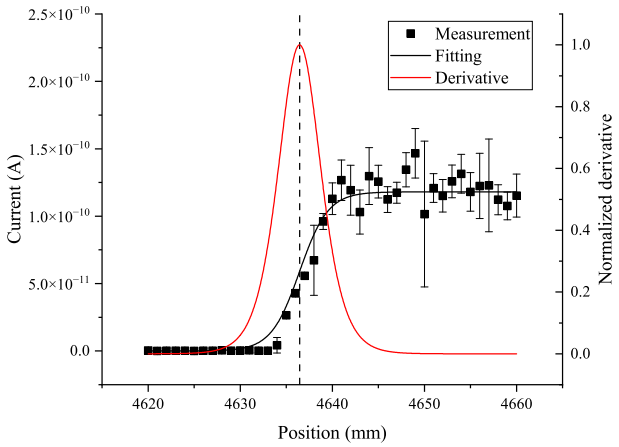

Fig. 7. Beam current measured using a beam profile monitor. The black closed squares and solid line represent the average current and a fitting curve with a sigmoid function. The red solid line indicates the derivative of the curve, which represents the beam profile. The dashed vertical line indicates the center of the beam profile.

with the current monitor. The average current was measured using the current monitor with a time constant of 30 seconds.

6. Results and discussion

The He^{2+} beam profile was measured in the radial direction using a beam profile monitor and beam probe to demonstrate charge exchange injection of the He^{2+} beam. The experimental results show that the injected He^{2+} beam circulated and reached the beam monitor.

The beam current along the radial axis measured using the destructive beam profile monitor, which was installed inside the injection section, is shown in Fig. 7. Figure 7 shows the measured current increase, which levels off at the position where the entire beam has been scraped. Therefore, the beam profile in the radial direction can be estimated by differentiating the measured current. Some measurements have large statistical errors as a result of fluctuation of the current intensity of the injected beam from the tandem accelerator. Assuming that the beam distribution is a Gaussian function, the beam profile (red solid line) was obtained by differentiating the curve obtained by fitting the measurements with a sigmoid function. The center position of the beam was 4637.2 mm. The current measured using the radial beam probe, which moves along a radial axis from outside of the accelerator, is shown in Fig. 8. Similarly, the obtained position of the beam was 4521 mm. The measurement error of the beam probe is relatively small since the averaging time of the signals is sufficiently larger than the fluctuation of the current intensity.

The horizontal size of the injected He^{2+} beam is expected to be 10 mm since the beam is scraped by the frame holding the carbon foil. The beam size as measured with the beam profile monitor and the beam probe was 9.6 ± 1.0 mm and 11.5 ± 0.2 mm, respectively. The distance between the designed orbit and the measured beam position at the beam profile monitor was 56 mm, and it was 27 mm at the beam probe. The experimental results indicate that the difference in position results from closed orbit distortion (COD) in the FFAG accelerator and the optical mismatch at the injection point. The RF cavity installed in the straight section of the accelerator disturbs the magnetic field and the closed orbit is distorted.

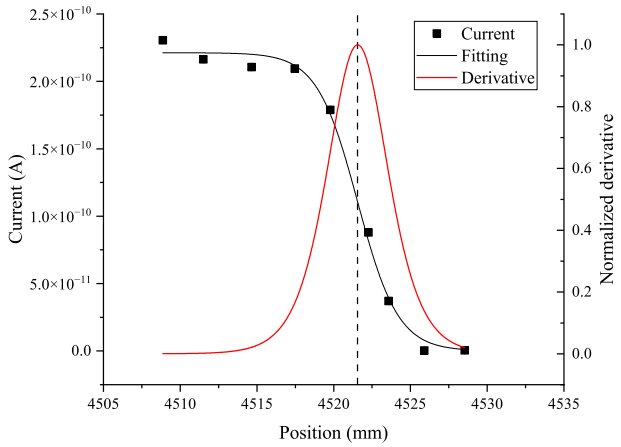

Fig. 8. Beam profile measured using a beam probe. The closed squares, black solid line, and red solid line represent the average current, the sigmoidal fitting curve, and the derivative of the curve, respectively. The dashed vertical line indicates the center of the beam profile.

Table 3. Measured beam position and designed beam position

	Beam probe	Beam profile monitor
Measured beam position x_m (mm)	4521.0	4637.2
Designed beam position x_d (mm)	4494.1	4693.0
COD (mm)	20	−35
$x_m - x_d -$ COD (mm)	7	−21

According to previous measurements [22], the COD at the beam probe and the beam profile monitor is estimated to be approximately 20 mm and −35 mm in the outward radial direction, respectively. The measured beam positions, designed beam positions, COD, and expected beam positions are summarized in Table 3.

Similarly, the injection orbit is distorted because the accelerator leakage field is magnetically coupled to the injection beam line. The difference in position between the designed orbit and the measured beam position at fluorescent screen B was 23 mm when the position of the charge-stripping foil was on the designed orbit. Investigation of the distortions of the closed and injection orbits of the He^{2+} beam caused by the leakage field, which decrease the injection mismatch, is a subject for future work.

7. Conclusion

A charge exchange injection method for positive heavy ions using the large momentum acceptance of an FFAG accelerator was proposed. As the first step to verify the injection method, an orbit shift from one charge state to the other is demonstrated. A charge injection system, which converts a He^{1+} beam to a He^{2+} beam, is developed for a 150 MeV FFAG accelerator at CABAS of Kyushu University. A 14 MeV He^{2+} beam circulated and reached the beam monitor. This is the first demonstration of heavy ion injection using an FFAG accelerator.

Acknowledgements

The authors thank Y. Ishi, T. Uesugi, and Y. Kuriyama of the Institute for Integrated Radiation and Nuclear Science, Kyoto University, for helpful discussions with regard to the charge-stripping foil. The authors also thank Y. Ishibashi, K. Kishimoto, W. Yamashita, K. Aradono, H. Matsuura, and Y. Tanaka of Kyushu University for construction of the beam transport line.

References

[1] Y. Mori, A. Taniguchi, Y. Kuriyama, T. Uesugi, Y. Ishi, M. Muto, Y. Ono, H. Okita, A. Sato, M. Kinsho, et al., JPS Conf. Proc. **21**, 011063 (2018). https://doi.org/10.7566/JPSCP.21.011063.

[2] H. Okita, A. Taniguchi, Y. Kuriyama, T. Uesugi, Y. Ishi, Y. Mori, M. Muto, Y. Ono, N. Ikeda, Y. Yonemura, et al., Nucl. Instr. Meth. Phys. Res. A **953**, 162988 (2020). https://doi.org/10.1016/j.nima.2019.162988.

[3] S. Naimi, H.F. Li, Y. Abe, Y. Yamaguchi, D. Nagae, F. Suzaki, M. Wakasugi, H. Arakawa, W. Dou, D. Hamakawa, et al., J. Phys. Conf. Ser. **1643**, 012058 (2020). https://doi.org/10.1088/1742-6596/1643/1/012058.

[4] T. Ohkawa, Proc. of the Annual Meeting of JPS, (1953).

[5] K. R. Symon, D. W. Kerst, L. W. Jones, L. J. Laslett, and K. M. Terwilliger, Phys. Rev. **103**, 1837 (1956). https://doi.org/10.1103/PhysRev.103.1837.

[6] M. Aiba, K. Koba, S. Machida, Y. Mori, R. Muramatsu, C. Ohmori, I. Sakai, Y. Sato, R. Ueno, et al., Proc. 7th European Particle Accelerator Conf. (EPAC 2000), 581 (2000).

[7] T. Adachi, M. Aiba, K. Koba, S. Machida, Y. Mori, A. Mutoh, J. Nakano, C. Ohmori, I. Sakai, Y. Sato, et al., Proc. 19th IEEE Particle Accelerator Conf. (PAC 2001), 3254 (2001).

[8] Y. Mori, Proc. 10th European Particle Accelerator Conf. (EPAC'06), 950 (2006).

[9] K. Okabe, R. Nakano, Y. Niwa, I. Sakai, Y. Ishi, M. Inoue, Y. Kuriyama, Y. Mori, T. Uesugi, J. B. Lagrange, et al., Proc. 1st Int. Particle Accelerator Conf. (IPAC'10), 3897 (2010).

[10] Y. Ishi, Y. Fuwa, Y. Kuriyama, H. Okita, H. Suga, T. Uesugi, and Y. Mori. Recent experimental results of the Accelerator Driven System with a sub-critical nuclear reactor (ADS) program. In: Proceedings of Cyclotrons' 19; 23–27 September 2019; Cape Town, South Africa(Geneva, Switzerland: JACoW Publishing; 2019), p. 7. https://doi.org/10.18429/JACoW-Cyclotrons2019-MOA01.

[11] S. L. Sheehy, D. J. Kelliher, S. Machida, C. Rogers, C. R. Prior, L. Volat, M. Haj Tahar, Y. Ishi, Y. Kuriyama, M. Sakamoto, et al., Prog. Theor. Exp. Phys. **2016**, 073G01 (2016). https://doi.org/10.1093/ptep/ptw086.

[12] M. Aiba, S. Machida, Y. Mori, A. Muto, J. Nakano, C. Ohmori, I. Sakai, Y. Sato, M. Sugay, A. Takagi, et al., Proc. 8th European Particle Accelerator Conference (EPAC 2002), 1076 (2002).

[13] Y. Yonemura, A. Takagi, M. Yoshii, Y. Mori, M. Aiba, K. Okabe, and N. Ikeda, Nucl. Instr. Meth. Phys. Res. A **576**, 294 (2006). https://doi.org/10.1016/j.nima.2006.11.072.

[14] Y. Yonemura, H. Arima, N. Ikeda, and Y. Mori, ICFA Beam Dynamics Newsletters **76**, 54 (2019).

[15] Opera-3d User Guide, Dassault Systèmes UK Ltd(Network House, Langford Locks, Kidlington, Oxfordshire, UK).

[16] K. Okabe, Y. Niwa, I. Sakai, Y. Ishi, Y. Kuriyama, Y. Mori, B. Qin, T. Uesugi, J. B. Lagrange, R. Nakano, et al., Proc. 2nd Int. Particle Accelerator Conf. (IPAC'11), 2676 (2011).

[17] J. F. Ziegler, M. D. Ziegler, and J. P. Biersack, Nucl. Instr. Meth. Phys. Res. B **268**, 1818 (2010).

[18] Y. Mori, Nucl. Instr. Meth. Phys. Res. A **562**, 591 (2006). https://doi.org/10.1016/j.nima.2006.02.044.

[19] D. Neuffer, Part. Accel. **14**, 75 (1983).

[20] T. Uesugi, Y. Ishi, Y. Kuriyama, and Y. Mori, Proc. 8th Int. Particle Accelerator Conf. (IPAC'17), 3747 (2017).

[21] J. B. Marion and F. C. Young, Nuclear reaction analysis (graphs and tables)(Amsterdam: North-Holland Publishing Company; 1968).

[22] Y. Yonemura, H. Arima, N. Ikeda, Y. Uozumi, K. Ishibashi, K. Sagara, T. Noro, T. Korenaga, Y. Inaoka, T. Miyaoki, et al., Proc. 10th Annual Meeting of Particle Accelerator Society of Japan, 852 (2013).